Fault Diagnosis for Methane Sensors using Generalized Regression Neural Network

http://dx.doi.org/10.3991/ijoe.v12i03.5443

Kaifeng Huang[1, 2], Zegong Liu[1], Dan Huang[3]
[1]Anhui University of Science and Technology, Huainan, China;
[2]Huainan Vocational and Technical college, Huainan, China;
[3]Huainan mining group co., LTD, Huainan, China;

***Abstract*—to identify the hang, collision and drift faults of methane sensors, this paper presents a fault diagnosis method for methane sensors using multi-sensor information fusion. A methane concentration monitoring approximation model with multi-sensor information fusion is established based on generalized regression neural network (GRNN). The output of the neural network is compared with the measured value of the sensor to be diagnosed to obtain the variation curve of the residual error signal. Through the analysis of the variation tendency of the residual error signal, the fault status of a methane sensor could be determined based on a reasonable threshold. Through simulation comparison is applied between the two models of GRNN and BP neural network; verify the GRNN model is much more precise in the approximation of methane concentrations. Fault diagnosis for methane sensors using generalized regression neural network is effective and more efficient.**

***Index Terms*—generalized regression neural network (GRNN), methane sensor, fault diagnosis, multi-sensor information fusion**

I. INTRODUCTION

Methane sensors are important detectors of methane concentrations under coal mine shafts. The performance of these sensors directly influences the safety of coal mines. The high levels of humidity and dust in underground coal mines frequently cause methane sensor faults, such as hang, collision, and drift faults. The prompt recognition of methane sensor faults is significant approach to ensure safety in coal mines. Therefore, studying methods for detecting methane sensor faults is crucial [1-2].

Artificial neural networks with self-learning ability, strong fault tolerance and excellent capability of parallel processing of information have been successfully used to diagnose and estimate faults in various fields. Khorasani et al. proposed a fault diagnosis and separation program based on a neural network. This program was designed for manual injection engine faults with high dynamic nonlinearity and was found to exhibit good fault diagnosis performance [3-4]. To diagnose flameout faults in diesel engines, Liu et al. [5] suggested to reduce the dimension of effective vibration signals with rough set and then established a back propagation (BP) neural network model to identify vibration signal patterns. Shao et al. [6] proposed a fault diagnosis method based on a global neural network to improve the stability and reliability of a proton exchange membrane fuel cell system. Their experimental result revealed that this method was superior to others in terms of fault diagnosis efficiency and generalizing ability. Rostek et al. [7] used a neural network to achieve an early detection and estimation of leakage faults in a fluid bed boiler. Their experimental result demonstrated that the neural network detected leakage faults effectively, and thus improving the fault classification system was possible. Zhu et al. and Xue et al. [8, 9] presented a fault prediction algorithm based on time-series using improved reservoir neural networks. B. Wang et al. developed a prediction and evaluation program that integrated a methane detector, neural network and methane diffusion model and was different from the real-time prediction and evaluation system of harmful methane diffusion. Their experimental verification revealed the high reliability of this system and its high correlation with the original evaluation model [10-13]. Zhang et al. [14] came up with a solution that combines artificial neural networks with fault tree analysis to improve the prediction of underground coal and methane outbursts. This solution provided effective references for predicting potential coal and methane outburst risks. In a study aimed at diagnosing faults in coal mines, Zhu et al. [15] established a chain wireless sensor network as a methane monitoring assistant with consideration of the geographic features of mine tunnels. Following the result of their analysis of the fault modes of methane sensors in coal mines, they proposed a methane sensor fault diagnosis technology based on chain wireless sensor networks. Complicated factors influence methane concentrations in coal mines. Hence, information fusion-based neural networks have become one of the main development directions of methane sensor fault diagnosis.

In the coal mine, the methane sensor worked in dreadful conditions, such as, obvious temperature fluctuations, high humidity, severe dust and strong electromagnetic interference. The close coupling between methane sensor and environment are determined by its structure and working principle. So, its output of monitoring data is mostly not dependent on historical data. Therefore, the fault diagnosis study in methane sensors isn't applied with fault diagnosis method which based on the time series. The traditional neural network has some problems such as slow convergence, network layers, no theoretical guidance on the choice of cell number and poor stability. By increasing the number of wireless sensors to build chain wireless sensor network, it can effectively improve the accuracy of fault diagnosis. But the cost of monitoring system will be increased greatly. In this paper, based on GRNN network, the data fusion technology of fault diagnosis is proposed. Assuming that each monitoring system has the same layout of sensor, the data fusion technology of fault diagnosis

can improve the convergence speed and stability of monitoring data by optimizing diagnosis prediction network and carrying out cross validation. Therefore, this technology has obvious advantages to improve the diagnosis accuracy without adding any sensor.

In the present study, a Generalized Regression Neural Network (GRNN) was employed for the high-accuracy approximation and estimation of methane concentrations. An estimation model based on a BP neural network was also established. Compared with the estimation model based on a BP neural network, the GRNN model had certain advantages in the construction of methane concentration approximation. Finally, we obtained a residual error between the estimated methane concentration of the GRNN model and the tested methane concentration. This error could reflect the working conditions of methane sensors on the basis of a reasonable threshold. As a result, methane sensor faults could be diagnosed.

II. FAULT DIAGNOSIS METHODS OF METHANE SENSOR

A. BP neural networks

BP neural network is widely applied in multiple sensor data fusion fault diagnosis. It is generally composed of an input layer, a hidden layer, and an output layer. The hidden layer can be one or more layers, and no node coupling exists in the same layer.

In a BP neural network, the input signal travels from the nodes of the input layer to the nodes of the hidden layer(s) and then to the nodes of the output layer. Such forward signal propagation is a layer-based updating process. The output status of the neuron nodes in the current layer is only influenced by the status of the neuron nodes in the previous layer. In back error propagation, a large error in the output layer may exist because the expected output node could not be acquired. Therefore, the weight and threshold of the neural network should be adjusted continuously through back error propagation until the output node of the output layer is approximate to the expected one. The objective of the learning process of the BP neural network is to train the network with training samples and to repeat both back error propagation and forward signal propagation. The weight of the BP neural network during back error propagation is adjusted according to delta learning rules. The inputs and outputs of the input layer, hidden layer(s) and output layer during forward signal propagation are calculated as follows:

$$w_i = \sum_j w_{ij} x_j + \theta_j$$

$$y = f(w_i) \tag{1}$$

Where w_i is the activation value of the ith node in one layer θ_j, is the threshold, x_j is the input signal. w_{ij} is the connection weight between the ith and jth nodes, and y_i is the output value of the ith node in one layer.

Back error propagation adjusts the weight and threshold according to error between the expected output and the actual output. The weight adjustment formula is shown in the following:

$$w_{ij}(t+1) = w_{ij}(t) - \eta \frac{\partial E}{\partial w_{ij}} \tag{2}$$

Where E is the neural network error between the expected output and the actual output, and η is the learning rate. The recognition or estimation result of a BP neural network is evaluated by using test samples once it meets the requirements after training.

B. Generalized Regression Neural Network

The GRNN was proposed by an American scholar in 1991, and it was developed from the Radial Basis Function (RBF) neural network. With strong nonlinear mapping and fitting capability, as well as high robustness, the GRNN can approximate hidden function relationships according to sample data. The GRNN has a simple structure and easy parameter adjustment during network training. The GRNN is superior to other neural networks in terms of approximation capability and learning speed. Moreover, it can overcome long convergence time and local minimum problems during prediction. It finally converges at the optimized regression surface with maintaining good prediction effect under the condition of small sample. As a result, the GRNN has been widely used in various industries, including finance control decision systems, bioengineering, and food science. The basic structure of the GRNN is shown in Figure 1.

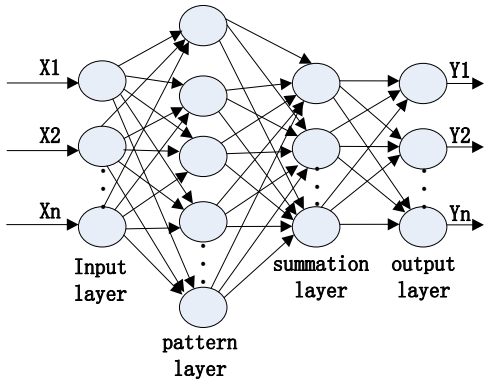

Figure 1. Structure of the GRNN

The GRNN consists of four layers namely: input layer, pattern layer, summation layer and output layer. Similar to the input layers of other neural layers, the input layer of the GRNN transmits input variables directly to the mode layer. The number of neurons in the input layer is equivalent to the dimension of the input vector in the forecast samples.

The number of neurons in the mode layer is equal to that in the input layer. Different samples correspond to different neurons. The neuron response function of the mode layer is:

$$P_i = \exp\left[-\frac{(X - X_i)^T (X - X_i)}{2\sigma^2}\right] \quad i = 1, 2, \mathrm{L}\ n \tag{3}$$

Where the output of neuron i is the exponential square of the Euclid distance square between the input variable and the corresponding sample, P_i is the output of neurons in the node layer, $D_i^2 = (X - X_i)^T (X - X_i)$, X is the input variable of the neural network, X_i is the learning sample corresponding to the ith neuron in the node layer; and σ is called the smoothing factor. Neuron summation in the summation layer can be divided into two types;

One neuron summation type is:

$$\sum_{i=1}^{n} \exp\left[-\frac{(X-X_i)^T(X-X_i)}{2\sigma^2}\right] \quad (4)$$

The weight between the neurons of the node layer and those of the summation layer Are all 1. All the outputs of the node layer are added. The summation transfer function is: $S_D = \sum_{i=1}^{n} P_i$.

Another neuron summation type is:

$$\sum_{i=1}^{n} Y_i \exp\left[-\frac{(X-X_i)^T(X-X_i)}{2\sigma^2}\right] \quad (5)$$

That performs a weighted summation of the outputs of the node layer. In formula (5), the *j*th element in (the *i*th output sample) is the connected weight of the sum between the *i*th neuron in the node layer and the *j*th neuron in the summation layer. The summation transfer function is:

$$S_{Nj} = \sum_{i=1}^{n} y_{ij} P_i \quad j = 1,2,\mathrm{L}\ k \quad (6)$$

The number of neurons in the output layer is equal to the final expected number of network tracking targets, that is, the output target vector dimensions in the forecast sample (k). The output of neuron j in the output layer corresponds to the jth element in the following estimation ($\hat{Y}(x)$):

$$y_j = \frac{S_{Nj}}{S_D} \quad j = 1,2,\mathrm{L}\ k \quad (7)$$

C. Cross-Validation method

Cross Validation (CV) evaluates the performance of a classifier by dividing the original data samples into training and validation sets. The training set is used to train and construct the classifier, whereas the validation set is used to verify the trained classifier model, which evaluates the performance of the classifier. CV is a statistical analysis method. Common CV methods include the hold-out method, K-fold CV (K-CV) and leave-one-out CV. In the present study, the K-CV method is applied. The original sample data are divided into K groups. Every group of data is viewed as one validation set and the remaining K-1 groups of data are used as a training set. After the circle training of the K combinations and the classifier verification, the mean classification accuracy under K validation sets is calculated as the final performance index of the classifier. Generally, K is valued at least 2. The K-CV method can avoid over-learning and under-learning and the classifier result is persuasive to a certain extent.

D. Methane sensor fault diagnosis model

The distribution of methane sensors on the coal face is shown in Figure 2. Figure 2 shows that temperature, CO, wind speed and volume as well as the methane concentrations at T_0 and T_2 are closely related to the measured value of T_1. The measured values of the corresponding sensors are used as the historical data sample for the offline training of the data fusion approximation. The approximation model of T_1 is established after it meets the preset training requirement. On the basis of this model, the data fusion approximation is constructed.

The methane sensor fault diagnosis model based on the GRNN approximation is shown in Figure 3. Based on the trained GRNN approximation, methane concentration (Y)

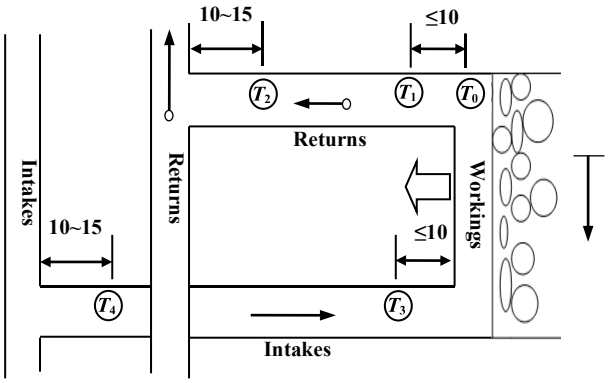

Figure 2. Methane sensor distribution on the coal face

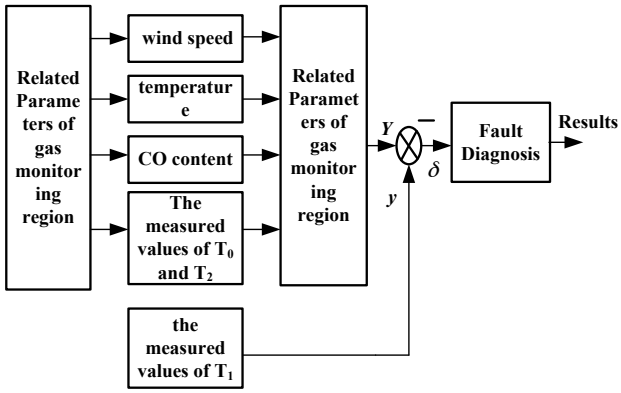

Figure 3. Methane sensor fault diagnosis model based on the GRNN approximation

is estimated by inputting temperature, CO, wind speed and the measured values of T_0 and T_2 into the neural network.

Y is used as the estimated value of T_1 is compared with the measured value (y) of T_1 to obtain the variation curve of the residual error signal, so that a fault in the methane sensor could be determined. If a small residual error between Y and y exists, then T_1 is operating normally. When the residual error between Y and y changes larger, the measured value (y) of the sensor (T_1) to be diagnosed cannot correctly determine the methane concentrations at the monitoring points, thereby T_1 is operating in fault state.

An appropriate fault diagnosis strategy for methane sensors allows the effective and timely detection of faults. The diagnosis strategy is as follows: the residual error of the methane sensor under normal operation conditions is consistent with white Gaussian noise characteristics, but it changes abnormally at faults. The waveform of the residual error will change significantly. Therefore, threshold can be set. $|y-Y| \geq \theta$, a methane sensor fault exists. However, a false alarm is sent if θ is significantly small and a leakage alarm is raised if θ is extremely high. This threshold is tested in practical engineering and finally determined to be 0.78.

III. VERIFICATION METHOD OF FAULT DIAGNOSIS FOR METHANE SENSORS

A. Site distribution of methane sensors

Safety monitoring systems in coal mines perform real-time methane concentration detections in the coal production environment through methane sensors (Right 1 in

Figure 4) and send the results to the monitoring center in real time (Figure 5). Through this process, the technical personnel can identify an accident risk according to current safety production conditions or field data statistics. The technical personnel can then adopt corresponding safety measures and avoid potential accidents. The ground data center can conduct dense monitoring at multiple points simultaneously. The minimum real-time data storage interval is 1 s. The intelligent KG9701 low-concentration methane sensor is used. Its main technical indicators are as follow: methane concentration measurement of 0%□4%, methane concentration measurement accuracy of ±0.10%□±0.30%, and signal output type represent as a frequency. The coal mine safety monitoring system is shown in Figure 6.

The methane sensor value at the test point (T_1) is related to the temperature, CO, wind speed and volume and measured values of the surrounding methane sensors (T_0, T_2). Related parameters could be integrated by establishing a methane concentration approximation based on data fusion. Such integration leads to highly accurate estimations of methane concentrations.

B. Training data and test data of GRNN acquisition

The input layer of the GRNN features five neurons, namely, wind speed, temperature, CO content, and the measured values of T_0 and T_2 near the monitoring points. Only one neuron exists in the output layer, that is, the approximation value of T_1 at the monitoring points. A total of 110 groups of on-site data are collected successively from the coal mine safety monitoring system as shown in the Figure 7. Each group of data includes wind speed, temperature, CO, and the measured values of T_0, T_2 and T_1. The five neurons in the input layer fluctuate in terms of order of magnitude.

To ensure the training effect of the neural network, the neurons are normalized first. Later, 110 groups of data are divided into two groups. The first 70 groups of data are used as the training data of the GRNN and the remaining 40 groups are used as the test data of the GRNN.

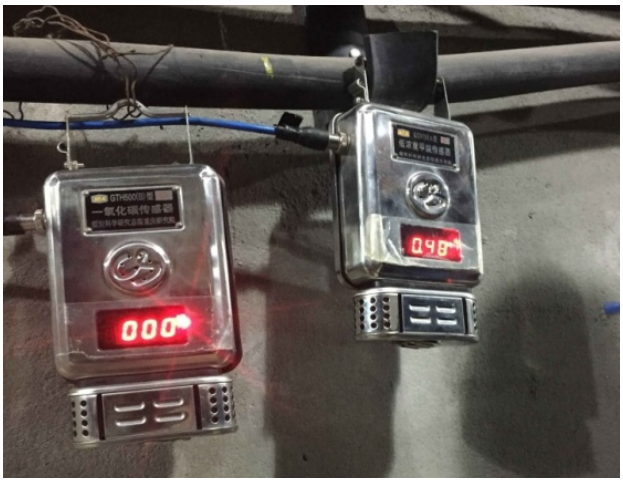

Figure 4. Site installation of methane sensors

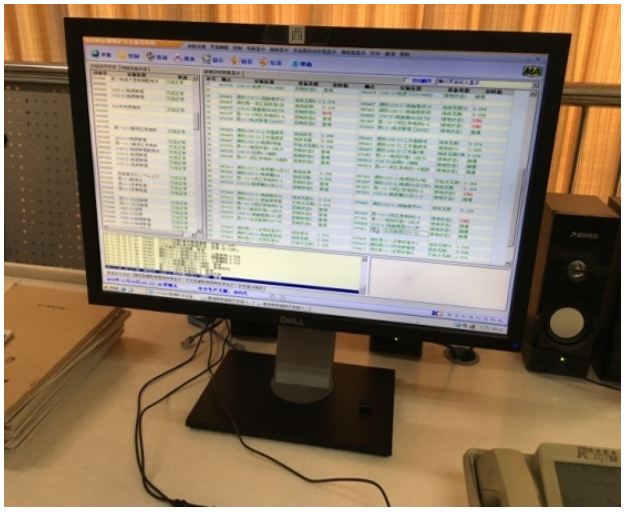

Figure 5. Monitoring platform at data center

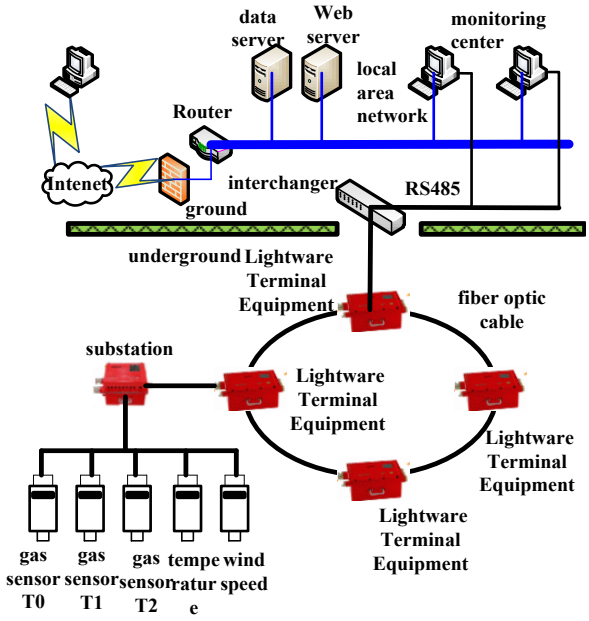

Figure 6. Safety monitoring system in coal mine

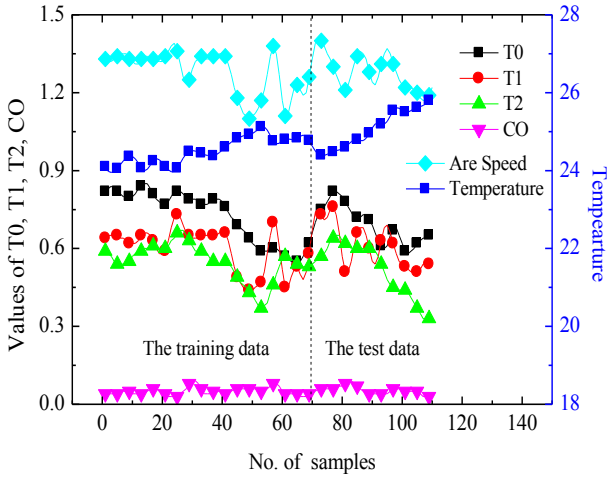

Figure 7. On-site data collection

C. *The comparison of approximation capability between the GRNN-based approximation and BP-based approximation*

Reasonably choosing the spread of the RBF in the GRNN is important. A minimal spread equates to the strong approximation capability of the GRNN. When the spread is high, the output curve of the GRNN exhibits good smoothness. However, the GRNN may reveal larger errors compared with the GRNN with minimal spread. To derive the best spread, the 70 groups of training data are divided into five groups with the K-CV method. One group is used as the test set, and the remaining four groups are used to train the GRNN. In this process, five cycle tests are performed. During each cycle test, from 0.1 to 2, the spread is substituted into the GRNN at a step length of 0.1 to test the network performance. Subsequently, the best spread can be gained to be 0.2.

The test data are applied on the trained GRNN. Figure 5 shows the mean square error (MSE) of the corresponding output of the GRNN under the best spread to be 2.8737e-04. The estimation is gained on the basis of 40 groups of test data. The estimations of a GRNN-based approximation and a BP-based approximation under the same test data and spread are compared (Figure 8). The output difference between the GRNN-based approximation and BP-based approximation under the same test data is shown in Figure 9.

An output difference exists between the GRNN and BP-based approximations under the same test data. As shown in Figure 6, the error of the GRNN-based approximation is limited within the range of [0, 0.15], whereas that of the BP-based approximation is limited within the range of [0, 0.25]. The error range of the GRNN is smaller than the BP neural network. Furthermore, the BP neural network model has to initialize a weight and threshold when it is used for sample forecast. It also features poor stability because of certain randomness, long convergence time and local minimum problems. On the contrary, the GRNN has a simple structure and involves few parameters for adjustment. It features fast estimation and good approximation capability in the selection of a correct spread.

D. *Results of methane sensor fault diagnosis*

In this paper, the simulation experiments were performed with four typical faults of methane sensor, [16] such as: collision, hang, drift and periodic fault. The collision fault was happening at the 32 sample, the hang fault was happening at the 30 sample, the drift fault was happening at the 32 sample, and the periodic fault was happening at the 17 and the 35 sample. The residual signal change curve was shown in Figure 10-13.

Figure 10-13 has shown that in comparing the estimation value Y and the measured value y, the variation curves of the residual error (δ) can be obtained if T_1 correspondingly acts once with collision, hang, drifting and periodic faults. When T_1 performs with the aforementioned faults, the residual error (δ) obtained in the comparison of Y and measured value y becomes higher than the preset threshold (0.78). The value of residual error signal was approximately zero, but it significantly increased when sensor fault. Through the results of simulation experiments has shown that, based on GRNN network the data fusion technology of fault diagnosis had an excellent diagnostic accuracy for drift fault and abrupt fault of the methane sensor.

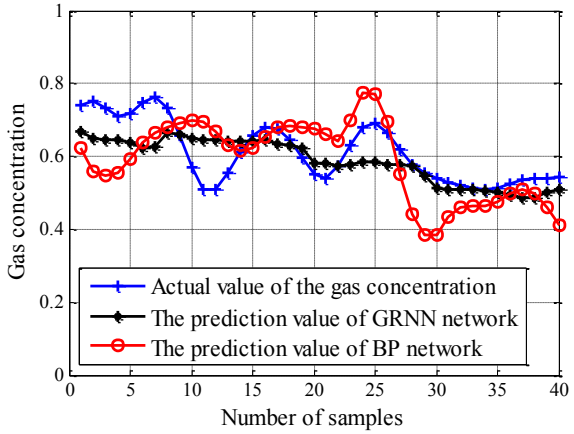

Figure 8. Estimations of GRNN and BP-based approximation

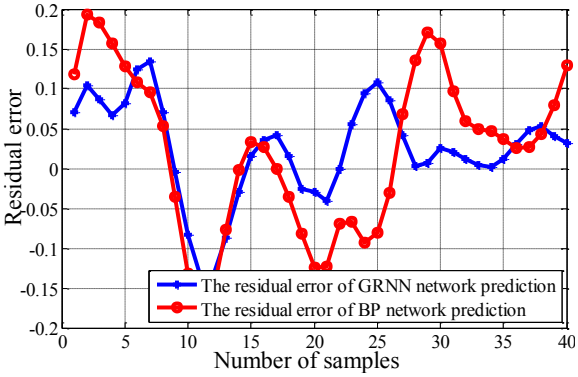

Figure 9. Residual error between GRNN and BP-based approximation

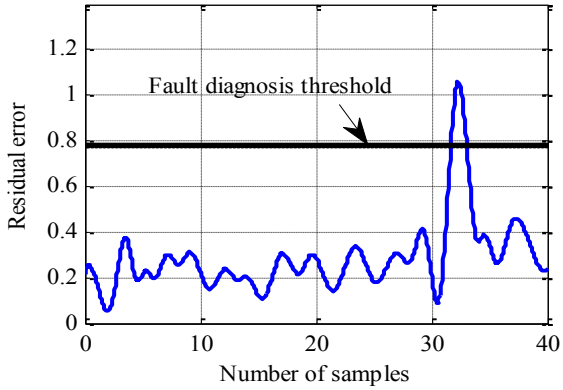

Figure 10. Residual error of the methane sensor at the collision fault

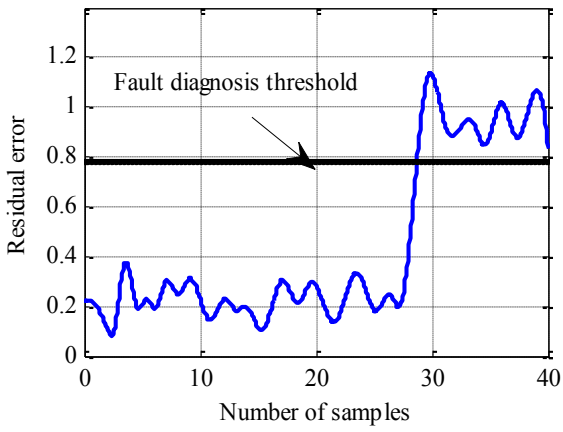

Figure 11. Residual error of the methane sensor at the hang fault

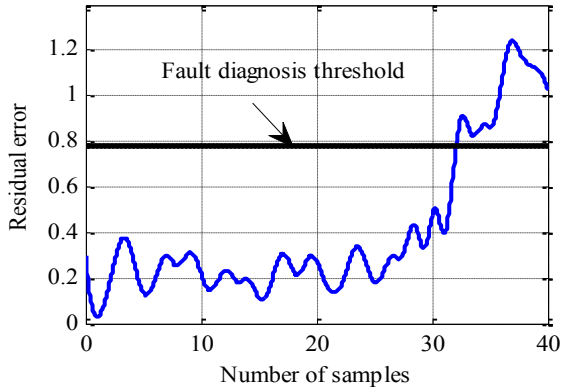

Figure 12. Residual error of the methane sensor at the drift fault

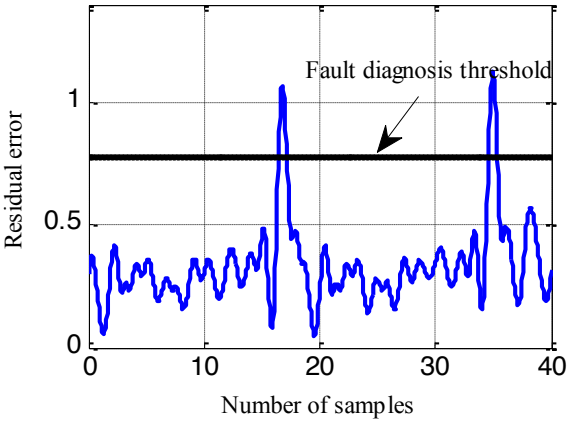

Figure 13. Residual error of the methane sensor at the periodic fault

IV. CONCLUSIONS

With a detailed analysis of the influencing factors of methane concentrations, the GRNN approximation is constructed for methane sensor fault diagnosis based on multi-sensor data fusion. The approximation value is used to determine whether a methane sensor is operating normally. The fault diagnosis of methane sensors is achieved by choosing an appropriate threshold.

A comparison is applied between the two models of GRNN and BP neural network. The Simulation results show that the proposed model is much more precise in the approximation of methane concentrations. Fault diagnosis for methane sensors using generalized regression neural network is effective and more efficient. The proposed fault diagnosis model is also applicable to other methane sensors except for T_1.

REFERENCES

[1] Wu S S, Huang Y R, Shi M, Wang F L, "Design of coal mine gas monitoring system based on wireless sensor networks. " *Coal Mine Machinery*, vol.33, no.5, pp. 240-241, July2012.

[2] Huang K F, Liu Z G, Wang Q J, Yang J, Gao K, "Gas sensor fault diagnosis based on ASGSO-SVR". *Journal of China Coal Society*, vol.38 (s2), pp.518-523, December 2013.

[3] Tayarani-Bathaie, S. Sina, Z N S. Vanini, K Khorasani, "Dynamic neural network-based fault diagnosis of gas turbine engines."*Neurocomputing,* vol.125, no.3, pp.153–165, February 2014. http://dx.doi.org/10.1016/j.neucom.2012.06.050

[4] Vanini, Z. N. Sadough, K. Khorasani, and N. Meskin, "Fault detection and isolation of a dual spool gas turbine engine using dynamic neural networks and multiple model approach." *Information Sciences* vol.259, no.3 pp.234-251, February2014. http://dx.doi.org/10.1016/j.ins.2013.05.032

[5] Liu J, Li X, Zhang X, Xu S, Dong L, "Misfire diagnosis of diesel engine based on rough set and neural network." *Procedia Engineering*, vol.16, no.16, pp.224-229, November 2011.

[6] Shao M, Zhu X J, Cao H F, Shen H F, "An artificial neural network ensemble method for fault diagnosis of proton exchange membrane fuel cell system."*Energy,* vol.67, no.4, pp.268–275. April 2014. http://dx.doi.org/10.1016/j.energy.2014.01.079

[7] Rostek K, Łukasz Morytko, Jankowska A, "Early detection and prediction of leaks in fluidized-bed boilers using artificial neural networks."*Energy*, vol. 89, pp.914-923, September 2015. http://dx.doi.org/10.1016/j.energy.2015.06.042

[8] Zhu Q, Jia Y, Peng D, Xu Y, "Study and application of fault prediction methods with improved reservoir neural networks." *Chinese Journal of Chemical Engineering*, vol. 22, no.7, pp. 812-819, July 2014. http://dx.doi.org/10.1016/j.cjche.2014.05.016

[9] Xue H D, Zhu Q X, "Time Series Prediction Algorithm Based on Structured Analogy." *Computer Engineering,* vol.36, no.1, pp.211-214, January 2010.

[10] Wang B, Chen B, Zhao J, "The real-time estimation of hazardous gas dispersion by the integration of gas detectors, neural network and gas dispersion models."*Journal of Hazardous Materials,* vol.300, no.30, pp. 433-442, December 2015. http://dx.doi.org/10.1016/j.jhazmat.2015.07.028

[11] Meysami H, Ebadi T, Zohdirad H, Minepur M, "Worst-case identification of gas dispersion for gas detector mapping using dispersion modeling." *Journal of Loss Prevention in the Process Industries*, vol.26, no.6, pp. 1407-1414. November 2013. http://dx.doi.org/10.1016/j.jlp.2013.08.019

[12] Pontiggia M, Derudi M, Alba M, Scaioni M, Rota R. "Hazardous gas releases in urban areas: assessment of consequences through cfd modelling." *Journal of Hazardous Materials*, vol.176, no.1-3, pp.589–596, April 2010. http://dx.doi.org/10.1016/j.jhazmat.2009.11.070

[13] Pontiggia M, Landucci G, Busini V, Derudi M, Alba M, Scaioni M, "Cfd model simulation of lpg dispersion in urban areas." *Atmospheric Environment*, vol.45, no.24, pp.3913-3923, August 2011. http://dx.doi.org/10.1016/j.atmosenv.2011.04.071

[14] Zhang R L, I S Lowndes. "The application of a coupled artificial neural network and fault tree analysis model to predict coal and gas outbursts."*International Journal of Coal Geology*, vol.84, no.2, pp.141-152, November 2010. http://dx.doi.org/10.1016/j.coal.2010.09.004

[15] Zhou G, Zhu Z, "Fault Diagnosis of Gas Sensor Based on Wireless Sensor Network." *Journal of Vibration Measurement & Diagnosis,* vol.30, no.1, pp.23-27, January 2010.

[16] Wang J H, Meng X R, Wu H W, "Gas sensor fault diagnosis based on wavelet packet and EKF-RBF neural network identification." *Journal of China Coal Society*, vol.35, no.5, pp.868-872, May 2011. (In Chinese).

AUTHORS

Kaifeng Huang is working with School of Energy and Safety, Anhui University of Science and Technology, and Information and Electrical Engineering Department of Huainan Vocational and Technical College, Huainan, 232001 China.(e-mail: kaifenghyj@163.com).

Zegong Liu is working with School of Energy and Safety, Anhui University of Science and Technology, Huainan, 232001 China. (e-mail: zgliu@aust.edu.cn).

Dan Huang is an Engineer in Huainan Mining Group Co., LTD, Huainan, 232001 China. (e-mail: 94609498@qq.com)

This research is funded by the National Natural Science Foundation of China (51304007) and Natural Science Fund of Education Department of Anhui province (KJ2015A376). Submitted 12 December 2015. Published as resubmitted by the authors 12 February 2016.